Shedding light on the binding mechanism of kinase inhibitors BI-2536, Volasetib and Ro-3280 with their pharmacological target PLK1

Jesús Fernández-Sainz[a], Pedro J. Pacheco-Liñán[a], José M. Granadino-Roldán[b], Iván Bravo[a], Jaime Rubio-Martínez[c], José Albaladejo[d] and Andrés Garzón-Ruiz[a,*]

[a] *Departamento de Química Física, Facultad de Farmacia, Universidad de Castilla-La Mancha, Cronista Ballesteros Gómez, 1, 02071, Albacete, Spain*

[b] *Departamento de Química Física y Analítica, Facultad de Ciencias Experimentales, Universidad de Jaén, Campus "Las Lagunillas" s/n, 23071 Jaén, Spain*

[c] *Departament de Ciència dels Materials i Química Física, Universitat de Barcelona (UB), Institut de Recerca en Quimica Teorica i Computacional (IQTCUB), Martí i Franqués 1, 08028 Barcelona, Spain*

[d] *Departamento de Química Física, Facultad de Ciencias Químicas, Universidad de Castilla-La Mancha, Avenida Camilo José Cela, 10, 13071 Ciudad Real, Spain*

*** Corresponding author:**

Professor Andrés Garzón Ruiz, Departamento de Química Física, Facultad de Farmacia, Universidad de Castilla-La Mancha, Cronista Ballesteros Gómez, 1, 02071, Albacete, Spain

Email: Andres.Garzon@uclm.es

Abstract

In the present work, the interactions of the novel kinase inhibitors BI-2536, Volasetib (BI-6727) and Ro-3280 with the pharmacological target PLK1 have been studied by fluorescence spectroscopy and molecular dynamics calculations. High Stern-Volmer constants were found in fluorescence experiments suggesting the formation of stable protein-ligand complexes. In addition, it was observed that the binding constant between

BI-2536 and PLK1 increases about 100-fold in presence of the phosphopeptide Cdc25C-p that docks to the polo box domain of the protein and releases the kinase domain. All the determined binding constants are higher for the kinase inhibitors than for their competitor for the active center (ATP) being BI-2536 and Volasertib the inhibitors that showed more affinity for PLK1. Calculated binding free energies confirmed the higher affinity of PLK1 for BI-2536 and Volasertib than for ATP. The higher affinity of the inhibitors to PLK1 compared to ATP was mainly attributed to stronger van der Waals interactions. Results may help with the challenge of designing and developing new kinase inhibitors more effective in clinical cancer therapy.

Key Words: PLK1; BI-2536; Volasertib; BI-6727; Ro-3280; Fluorescence spectroscopy; Molecular modelling

1. Introduction

Polo-like kinases (PLKs) are a conserved subfamily of serine/threonine kinase proteins which are widespread in eukaryotic cells [1–3]. In humans, this subfamily of proteins includes five members (PLK1-5) being PLK1 (also known as STPK13) the best-characterized and most investigated [4–6]. This kinase plays a crucial role in diverse mitotic events such as mitotic entry, spindle formation, chromosome segregation, DNA replication and cytokinesis, among others [7–10]. PLK1 is therefore essential for regulating the cell division and maintaining genome stability during mitosis, spindle assembly and DNA damage response [5,11]. Diverse studies have shown that this protein is overexpressed in many human cancers and is often associated to a poor prognosis [12–15]. Inhibiting its activity reduces proliferation in a broad range of cancer cell lines, highlighting PLK1 as an attractive drug target for cancer therapy [16–18].

Human PLK1 is formed by an N-terminal kinase domain (KD; residues 49-310) and a C-terminal region containing the polo box domain (PBD; residues 345-603), both connected by an inter-domain linker (IDL) [4,19]. KD is highly conserved and contains an ATP-binding site, a T-loop (whose phosphorylation is directly related to the kinase activity of PLK1) and a hinge region [4,19]. Autoinhibited PLK1 can be activated through phosphorylation of Thr210, at the T-loop [20–23], or of Ser137, at the end of the hinge region [23–25]. Besides, the protein can also be activated by a phosphopeptide binding to the regulatory domain, PBD [11,20,25–28]. Diverse phosphopeptides containing the Ser-pThr motif can bind to the PBD [29]; for example, the target sequence peptide Leu-Leu-Cys-Ser-pThr-Pro-Asn-Gly-Leu from Cdc25C phosphatase (Cdc25C-p), a natural substrate of PLK1 [30,31]. Therefore, the conformational plasticity seems to be crucial to the kinase activity of PLK1. The linker region L1 of the PBD docks into a concave surface of the KD (formed by the β1 strand of the N lobe, the helix αD of the C lobe and the hinge region) inhibiting its activity, while the binding of the PBD to the phosphorylated target can disrupt the intramolecular interaction between both domains [4].

Both the ATP pocket at the catalytic domain of PLK1 and the phosphopeptide binding pocket at PBD are being investigated as target sites for the development of new antitumor drugs [32]. In the last years, several ATP-competitive inhibitors of PLK1 with promising antitumoral activity have emerged, some of them reaching a clinical phase [17,32], whereas only a few nonpeptidic inhibitors targeting PBD have been identified so far [33–36]. The present work is focused on three ATP-competitive clinically tested kinase inhibitors, i.e. BI-2536, Volasertib (BI-6727) and Ro-3280 (see Fig. 1). BI-2536 and Volasertib are two dihydropteridinone derivatives developed by Boehringer Ingelheim Inc. which exhibit a potent activity against PLK1 in vitro (IC_{50} = 0.83 and 0.87 nM for BI-2536 and Volasertib, respectively) [17,32]. Crystallization studies revealed

that the pteridinone moiety of both derivatives is placed in the adenine portion of the ATP pocket, with the N-methyl-piperidine group (BI-2536) or N-(Cyclopropylmethyl)piperazine group (Volasertib) pointing to the solvent [32,37,38]. BI-2536 causes perturbation of the spindle assembly, leading to mitotic arrest and subsequent apoptosis, but it also inhibits other Polo-like kinases such as PLK2 (IC_{50} = 3.5 nM) and PLK3 (IC_{50} = 9 nM) [32,39,40]. Three phase II studies with patients with non-small cell lung cancer, advanced pancreatic cancer, or hormone-refractory prostate cancer, have also been completed with this kinase inhibitor [41–43]. Recently, a high affinity of BI-2536 for human serum albumin (HSA) has been observed [44], which could lead to a reduced concentration of free drug in the blood plasma. On the other hand, this arises as an excellent opportunity to develop new HSA-based delivery systems to target BI-2536 to solid tumors that use HSA as an energy source and accumulate this protein within the tumor interstitium [45–47]. The other selected dihydropteridinone derivative, Volasertib, induces the formation of monopolar spindles and a distinct prometaphase arrest phenotype (polo-arrest) and subsequent apoptosis [17,32]. This compound also inhibits PLK2 (IC_{50} = 5 nM) and PLK3 (IC_{50} = 56 nM) and is active against a broad range of *in vitro* tumor cells [17,32,48]. Volasertib shows favorable pharmacology, is well tolerated [17] and has reached the clinical phase III (in combination with subcutaneous low-dose cytarabine) for the treatment of acute myeloid leukaemia [49]. Both BI-2536 and Volasertib are also BET (bromodomain and extra terminal) inhibitors [50–52] and have shown promising results in HIV "shock and kill" therapy because they significantly reactivate silenced HIV-1 provirus at both the mRNA and protein level [53]. The third selected kinase inhibitor, Ro-3280, is a pyrimidodiazepine derivative developed by Hoffmann-La Roche Inc. [54]. This compound is also a potent ATP-competitive inhibitor of PLK1 although its enzymatic IC_{50} (3 nM) is somewhat higher than the IC_{50} values

measured for BI-2536 and Volasertib but, on the contrary, Ro-3280 has nearly no effect on PLK2 and PLK3 [54,55]. This pyrimidodiazepine derivative induces apoptosis and cell cycle disorder in leukemia cells, and has been proposed as a suitable drug candidate for the treatment of pediatric acute myeloid leukemia [55]. Unfortunately, no crystallographic data have been reported to date for the complex of PLK1 with Ro-3280.

Thus, it is assumed that the efficient interaction of BI-2536, Volasertib and Ro-3280 with PLK1 is directly related to their pharmacological activity, and there is a lack of knowledge about the mechanism and magnitude of such association process. In this sense, the overall aim of this work is to shed light on these issues by fluorescence spectroscopy experiments and molecular dynamics (MD) calculations. Protein-ligand interaction experiments were carried out in solution and their results are a valuable complement to the information extracted from crystallographic data. The intrinsic fluorescence of proteins, mainly due to tryptophan or tyrosine, is highly sensible to its local environment. Changes in the emission spectra of the fluorophores often occur in response to conformational transitions, subunit associations, substrate binding or denaturalization [56]. Here, fluorescence spectroscopy was employed to delve into the binding processes between PLK1 and the kinase inhibitors as well as to analyze the effect of Cdc25C-p on the affinity of these compounds to PLK1. MD has allowed to rationalize some experimental observations such as the higher affinity of PLK1 to BI-2536 and Volasertib than to its natural substrate. Finally, the main intermolecular interactions involved in the binding process between these kinase inhibitors and the proteins are discussed.

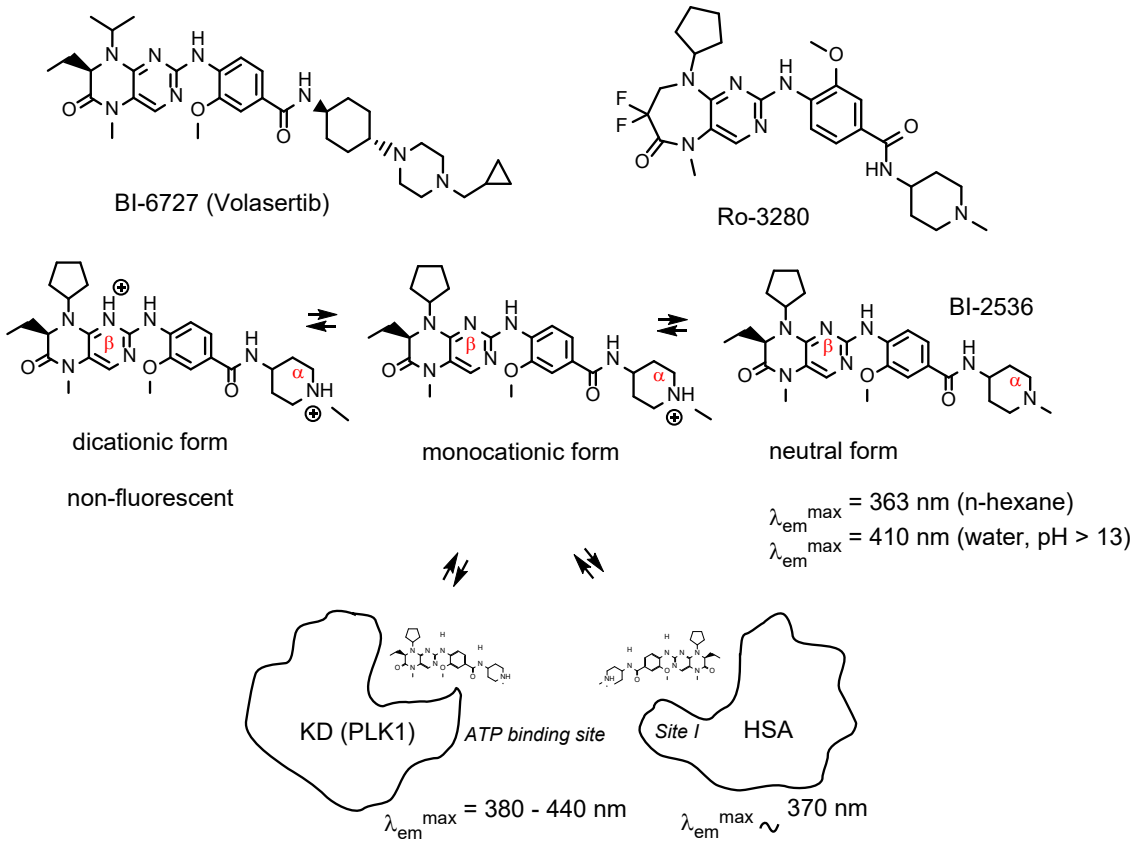

Fig. 1. Chemical formulae of the selected kinase inhibitors, i.e. Volasertib, BI-2536 and Ro-3280. Different protonation states of BI-2536 are shown. Fluorescence emission maximum wavelengths (λ_{em}^{max}) of BI-2536 in neutral form are also collected (λ_{em}^{max} of BI-2536 is similar in monocationic form and in neutral state) [44].

2. Material and methods

2.1. Chemicals and solutions

BI-2536 (purity ≥ 99.5%), BI-6727 (Volasertib) (purity ≥ 99.5%) and Ro-3280 (purity ≥ 99.5%) were supplied by MedChem Express. PLK1 (Human Myc-DDK-tagged ORF Clone) (purity > 80%) were supplied by Origene Technologies. The phosphopeptide Cdc25C-p (purity 96.5%), with sequence Leu-Leu-Cys-Ser-pThr-Pro-Asn-Gly-Leu was synthetized by Destina Genomics.

For binding experiments, working solutions of PLK1 were daily prepared in 0.02 M Tris-HCl buffer solutions at pH 7.4 containing 0.1 M NaCl. Bis-Tris (Sigma) and NaCl (Panreac) had a purity of ≥ 99.0%. Water was purified in a Mili-Q System (Millipore).

The solvents employed for the stock solutions of the kinase inhibitors were ethanol (for BI-2536 and Volasertib) and dimethyl-sulfoxide (for Ro-3280).

2.2. Spectroscopy measurements

4×10 mm quartz cuvettes were employed for the spectroscopic experiments. The UV–vis absorption spectra were recorded using a Cary 100 (Varian) spectrophotometer with a step of 1 nm and at room temperature. Steady-state fluorescence spectra of the samples were recorded employing a FLS920 (Edinburgh Instruments) spectrofluorometer equipped with a Xe lamp of 450 W as light source and a MCP-PMT (microchannel plate-photomultiplier tube) detector (R3809 model). The temperature of the sample was kept constant using a TLC 50 temperature-controlled cuvette holder (Quantum Northwest). FLS920 spectrofluorometer is also equipped with two polarizers placed in the excitation and emission light pathways which were employed for fluorescence anisotropy measurements. Polarized emission spectra were recorded at four polarizer directions, i.e. both horizontal (HH), both vertical (VV), horizontal on excitation and vertical on emission (HV) and vice versa (VH). The anisotropy spectra were calculated as

$$r = \frac{F_{VV} - F_{VH}}{F_{VV} + 2F_{VH}} \quad (1)$$

where F_i is the fluorescence intensity at the corresponding configuration of the polarizers.

2.3. Binding experiment conditions

800 μL of a working solution of PLK1 (0.1 μM) was titrated by successive additions of a stock solution of kinase inhibitor (60 μM). The final concentration of kinase inhibitor in the titration was 2.0 μM (the [ligand]:[protein] ratios were 0, 1, 3, 5, 10, 15, and 20). The

added volume of kinase inhibitor solution to the working solution of protein was 27.6 µL. The temperature of the sample was kept constant at 310 K.

The chosen excitation wavelength was 275 nm (8 nm slit) and the emission fluorescence intensity was collected at 296 nm (3 nm slit). In such conditions, the fluorescence signal comes from tyrosine residues without a significative contribution of tryptophan residues. On the contrary, the fluorescence emission spectra upon excitation at wavelength ≥ 285 nm has a certain contribution from tryptophan residues (see Fig. S1b) but the signal intensity drops significantly (see Fig. S1a). Here, it should be considered the scarcity of tryptophan residues in the protein (for instance, the kinase domain has a single tryptophan and nine tyrosine residues; see Fig. 2a) and the high dilution of the sample (the working concentration of 0.1 µM is low in comparison with the concentration of 1-15 µM typically used in other fluorescence quenching studies reported for lower-cost proteins such as albumin, hemoglobin, trypsin, lysozyme, catalase, among others) [44,57–62] [(a) Rahman 2021 https://doi.org/10.1016/j.molliq.2021.117144 ; (b) Rahman 2021 https://doi.org/10.1016/j.saa.2020.118803 ; (c) Ojha 2012 http://dx.doi.org/10.1016/j.tca.2012.08.016]

The emission fluorescence from PLK1 was corrected for the inner filter effect through

$$F_{corr} = F_{obs}\, 10^{(A_{ex}+A_{em})} \qquad (2)$$

where F_{corr} and F_{obs} are the corrected and observed fluorescence intensities, and A_{ex} and A_{em} are the absorbance of the system at excitation and emission wavelengths (275 and 296 nm, respectively) [56].

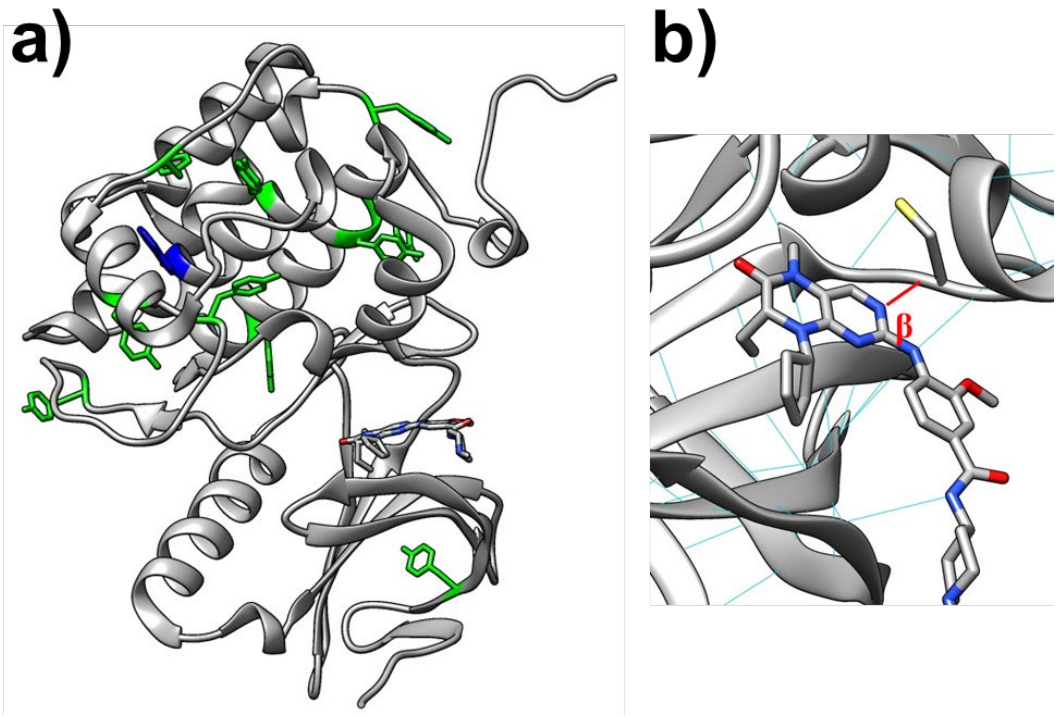

Fig. 2. (a) Kinase domain of PLK1 showing the tyrosine residues (green), the single tryptophan residue (blue) and the ligand (BI-2536) placed in the ATP-site (cyan). (b) H-bonds established between BI-2536 and PLK1 (the H-bond between the group $=N_{\beta}-$ of BI-2536 and Cys133 is highlighted in red). Source Protein Data Bank (PDB): 2RKU [37].

2.4. Computational details

To the best of our knowledge, no full-length human PLK1 crystal structure is available in the Protein Data Bank, although the separate structures of the KD [63] and PBD [19,26,29] have already been deposited. Thus, we used as initial structures for our computational analysis those available structures of the KDs with each ligand bound. Unfortunately, no structure of Ro-3280 bound to PLK1 KD is available up to date, so we decided to set aside that ligand from the theoretical study. Besides, some additional modeling was needed (see below) to obtain an initial structure for the PLK1/ATP system, as the experimental structure available was that for a zebrafish PLK1 bound with ADP.

The calculations herein reported were accomplished with the CUDA version of the pmemd module of Amber v18 suite [64], using the Amber ff14SB force field [65]. Trajectory post-processing and clustering was performed with the cpptraj module, while

the binding free energy was estimated with the MMPBSA.py [66] program, both included in the Amber v18 suite. An alternative binding free energy was obtained by means of the K_{DEEP} [67] web application. Figures were rendered with UCSF Chimera [68]. Hydrogen bonds were assigned with cpptraj or Chimera using their default options, with no relaxation of constraints.

2.4.1. Preparation of PLK1-ligand complexes

The three-dimensional structures of the human PLK1 KD complexed with BI-2536 and Volasertib, together with that of the zebrafish KD PLK1 complexed with ADP were retrieved from the Protein Data Bank (www.rcsb.org/pdb), with codes 2RKU [37], 3FC2 [38] and 3D5W, respectively [69]. The protonation states for all the residues were predicted with the ProteinPrepare web application [70]. The parameters for ligands were obtained using the general amber force field [71]. Charges were generated with the restrained electrostatic potential [72] at the HF/6-31G* level for BI-2536 and Volasertib, while, taking into account its high negative charge, HF/6-311+G(d,p) was used for ATP. The initial model for the human PLK1/ATP complex was obtained by superimposing the 3D5W structure on the 2RKU one to place the ADP ligand. Then, the ATP from a structure of the kinase Aurora A in complex with ATP [73] (PDB code 5DN3) was superimposed to the ADP of the 2RKU/ADP complex to replace ADP with ATP.

All the initial structures were processed with the LeAP program of the Amber v18 suite, where the systems were soaked in a cubic box, using TIP3P [74] explicit water molecules with periodic boundary conditions.

2.4.2. Molecular dynamics

Minimization and equilibration were done as described elsewhere [75], with two differences: first, the number of cycles of each of the steps of minimization was doubled in the case of the PLK1/ATP complex; and second, the cut-off used for the non-bonded interactions was increased to 10 Å. Then, ParmEd [64] was used to modify each topology in order to use hydrogen mass repartitioning [73], and thus an additional equilibration step of 100 ns (200 ns for the PLK1/ATP complex) in the NVT ensemble, with an integration step of 4 fs, was conducted to use the last snapshot of this trajectory as starting point to perform 5 runs of 100 ns of MD [76].

2.4.3. Clustering

In order to identify different possible conformations explored during the MD runs, two different families of clusters were obtained using the dbscan algorithm [77]. This clustering algorithm needs two parameters, namely *mindist* and *epsilon*, which have been obtained plotting a so-called K-dist plot for *kdist* values ranging from 1 to 10. Once the best parameters are found, two distance metrics were used, the first one used the best-fit coordinate RMSd using as mask all C_α atoms, whilst the second one used the coordinates of all the atoms in each binding pocket (each binding pocket was defined, using each initial structure, with those residues of PLK1 being at a distance of 3.6 Å or less from any atom of each ligand). Only those clusters with a number of members equal or higher than 20% of the most populated clusters were further analyzed. The structures of the representatives of each cluster found (clustering of structures) can be downloaded as `data in brief´.

2.4.4. QM-MMGBSA calculations

A total of 1000 frames for each of the 5 MD trajectories obtained were used for QM-MMGBSA binding free energy calculations. The following equation was used to obtain the binding free energy for each frame, which was later averaged over all the frames analyzed:

$$\Delta G_{bind} = \Delta E_{MM} + \Delta E_{SCF} + \Delta G_{solv} - T\Delta S \quad (3)$$

where the molecular mechanics term, ΔE_{MM}, includes contributions from bonded (bond, angle, dihedral) and nonbonded (electrostatic, ΔE_{EEL}, and van der Waals, ΔE_{vdW}). Besides, ΔG_{solv} is composed by a polar (ΔG_{GB}) and a nonpolar (ΔG_{SURF}) terms. For the polar term, we have chosen to use the generalized Born (GB) method [78], concretely the Hawkins, Cramer and Truhlar [79] generalized Born method (igb = 1). The nonpolar term was calculated using the following equation:

$$\Delta G_{SURF} = \gamma SASA + \beta \quad (4)$$

where SASA stands for the solvent-accessible surface area, calculated using the linear combinations of pairwise overlaps (LCPO) method [80], whilst the values used for γ and β were 0.0072 kcal mol^{-1} Å^{-2} and 0 kcal mol^{-1}, respectively [81]. Finally, ΔE_{SCF} encompasses the energy of the atoms in the Quantum Mechanics (QM) zone (defined as the atoms of each ligand), which in this case is calculated using the PM6 [82] semiempirical Hamiltonian. Thus, ΔE_{EEL} has to be zero in this case, while the ΔE_{SCF} term would account for the difference in electrostatic interactions between the ligand bound to the protein and the free ligand, under the one-trajectory approximation used here. Due to the high computational cost and our aim of using the calculated data with comparative purposes, the entropic term was not taken into consideration.

3. Results and discussion

3.1. Effect of Cdc25C-p on the affinity of PLK1 to BI-2536

The addition of increasing quantities of BI-2536 to a PLK1 solution quenched the fluorescence emission of the protein (see Fig. S2). Similar behavior was observed when the phosphopeptide Cdc25C-p is present in the reaction medium at 1:1 stoichiometric PLK1 ratio (see Fig. 3a). In both experiments, a weak emission band with an isosbestic point at ~370 nm emerges upon BI-2536 titration indicating the formation of a new fluorescent species. In a previous work, it was reported that the drug has a maximum fluorescence emission between 363 and 428 nm in different organic solvents but the fluorescence signal disappears in aqueous solution at physiological pH [44]. Under these conditions, BI-2536 is present mainly in dicationic form and only when dihydropteridinone moiety losses a proton (from $=N_{\beta}H^{+}-$ group, see Fig. 1) at higher pH values the fluorescence is restored [44]. Interestingly, the fluorescence of BI-2536 was also observed in presence of HSA what suggests that the drug binds to the site I of the protein in monocationic form [44]. For complex PLK1/BI-2536, the reported crystal structure (see Fig. 2b) [37] along with theoretical calculations (*vide infra*) showed that the dihydropteridinone moiety stay in neutral form where the lone pair of electrons on $=N_{\beta}-$ group are able to form a hydrogen bond with Cys133. Consequently, the fluorescence of BI-2536 is observed in presence of the protein.

Negative deviations of the Stern-Volmer plots were found for the BI-2536 titration experiments, both in presence and absence of Cdc25C-p (see Fig. 3b). In proteins, this behavior is typically associated to the presence of inaccessible fluorophores [83]. A linear trend was observed employing a modified Stern-Volmer equation which takes account the fraction of fluorophores that is accessible to the quencher, *f*:

$$\frac{F_0}{(F_0 - F)} = \frac{1}{f} + \frac{1}{f\,K_{SV}}\left(\frac{1}{[Q]}\right) \qquad (5)$$

where F_0 and F are the fluorescence intensity of the protein in the absence of ligand (quencher) and at a given concentration of ligand, respectively; and [Q] is the quencher

concentration (see Fig. 3c). The value of $f = 0.27$ obtained in the titration experiments indicates that not all tyrosine residues are accessible to BI-2536 (see Table 1). Interestingly, the fraction of accessible fluorophores to the drug slightly increases in presence of Cdc25C-p. The large values obtained for K_{sv} (in the order of 10^6 M^{-1} s^{-1}) cannot be totally associated to a dynamic quenching mechanism and suggest the formation of stable protein-ligand complexes (static quenching) [84]. This is more clearly revealed when the bimolecular quenching rate constant, k_q, is calculated by equation 4

$$k_q = K_{SV} / \tau_0 \quad (6)$$

where τ_0 is the fluorescence lifetime of the protein. Fluorescence lifetimes between 4.0 and 5.5 ns have been reported for different proteins when excited within 275 – 280 nm (λ_{em} = 318 – 320 nm; in that conditions, the monitored fluorescence signal comes mainly from tyrosine residues) [85,86]. Thus, k_q values in the order of 10^{14} M^{-1} s^{-1} were estimated for the fluorescence quenching experiments of PLK1 considering a tentative fluorescence lifetime of 5.0 ns. The diffusion-limited rate constant in water (~10^{10} M^{-1} s^{-1}) is notably lower than the estimated value for k_q showing the large contribution of the formation of protein-ligand complexes to the fluorescence quenching mechanism [56].

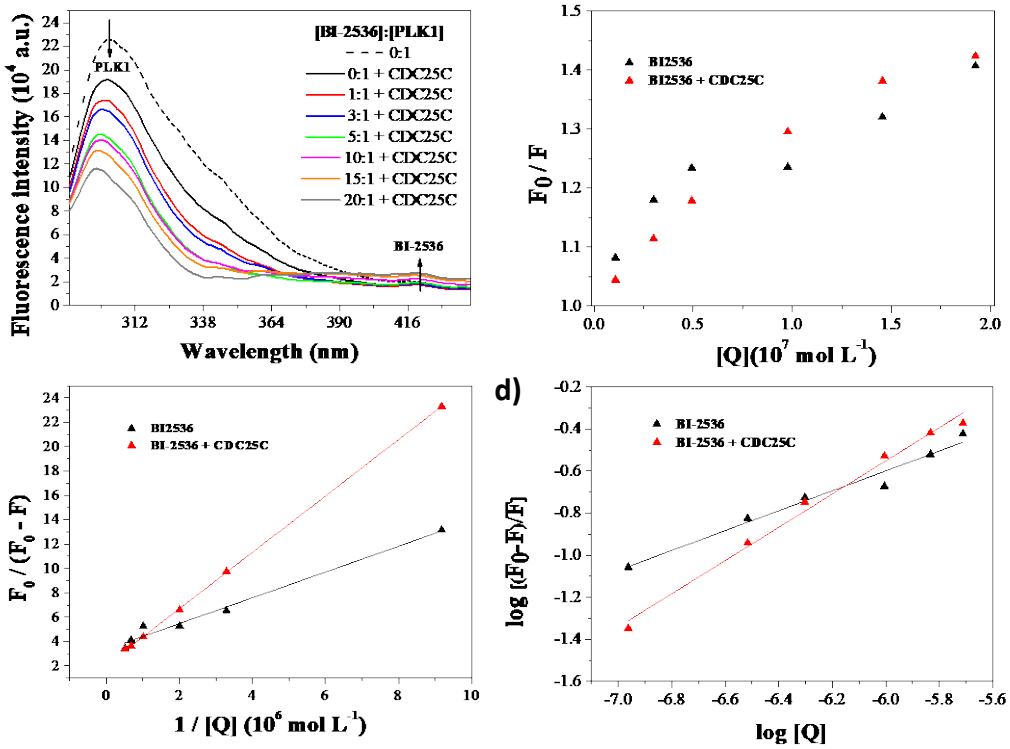

Fig. 3. a) Effect of BI-2536 on the fluorescence emission spectrum of PLK1, along with Cdc25C-p in 1:1 stoichiometric proportion (T = 310 K, λ_{ex} = 275 nm). [PLK1] = [Cdc25C-p] = 0.1 μM; [BI-2536] = 0.1–2.0 μM. b) Stern-Volmer plot in presence and absence of Cdc25C-p. c) Modified Stern-Volmer plot according to equation 5 in presence and absence of Cdc25C-p. d) Plot of log [(F_0 − F) / F] *vs.* log [Q] according to equation 7 in presence and absence of Cdc25C-p.

Once established that protein-ligand complexes are formed, the binding constant, K_a, was obtained by using the following equation:

$$\log\left(\frac{F_0-F}{F}\right) = \log K_a + n\, log[Q] \qquad (7)$$

where *n* is the number of binding sites [87–89] [(a) Rahman 2021 https://doi.org/10.1016/j.molliq.2021.117144 ; (b) Rahman 2021 https://doi.org/10.1016/j.saa.2020.118803 ; (c) Ojha 2012 http://dx.doi.org/10.1016/j.tca.2012.08.016]. Good linearity was observed in all the titration experiments as is shown in Fig. 3d, (results of the fit according to equation 7 are listed in Table 1). The binding constant between BI-2536 and PLK1 increases two orders of magnitude in presence of Cdc25C-p, with the number of binding sites close to unity. This finding agrees with the reported mechanism in which the activating phosphopeptide

binds to PBD releasing the KD domain and, therefore, the ATP-site should be more accessible to the drug [16,30,31]. Nevertheless, the rotational diffusion of the protein is not very sensitive to the presence of the activating phosphopeptide and the drug (see Table 2), and no major structural modifications are expected for PLK1 when it binds to Cdc25C-p and BI-2536 since the fluorescence anisotropy of the protein showed weak dependence upon addition of those compounds (see Table 2).

Table 1
Stern–Volmer quenching constant, K_{SV}, and accessibility factor, *f*, obtained from equation 5, along with protein-ligand binding parameters obtained from equation 7. Cdc25C-p column indicates the absence (No) or presence (Yes) of the phosphopeptide in the reaction medium (in a 1:1 stoichiometric ratio with with PLK1). The temperature of the experiments was 310 K.

Ligand	Cdc25C-p	$K_{SV} \pm 2\sigma$ (10^6 M^{-1})	$f \pm 2\sigma$	$n \pm 2\sigma$	Log $K_a \pm 2\sigma$	K_a (10^3)
BI-2536	No	4.49 ± 2.45	0.27 ± 0.11	0.46 ± 0.03	2.20 ± 0.07	0.158
BI-2536	Yes	1.38 ± 1.89	0.34 ± 0.20	0.80 ± 0.02	4.19 ± 0.10	15.5
Volasertib	Yes	2.84 ± 4.82	0.29 ± 0.15	0.80 ± 0.07	4.18 ± 0.42	15.2
Ro-3280	Yes	2.18 ± 1.59	0.28 ± 0.04	0.71 ± 0.04	3.63 ± 0.24	4.30
ATP	Yes	3.25 ± 4.33	0.33 ± 0.14	0.65 ± 0.02	3.38 ± 0.04	2.40

Table 2
Fluorescence excitation anisotropy, *r*, recorded at 275 nm for PLK1 in presence of different concentrations of BI-2536. [BI-2536]:[PLK1] indicates the concentration ratio between the ligand and the protein. The experiments 1 and 2 were carried out in absence and presence of Cdc25C-p, respectively.

	r	
[BI-2536]:[PLK1]	Experiment 1	Experiment 2 (Cdc25C-p)
0:1	0.123	0.133
1:1	0.137	0.140
3:1	0.143	0.138
5:1	0.154	0.150
10:1	0.152	0.145

3.2. Binding experiments of PLK1 to the selected kinase inhibitors

Once established the crucial role of Cdc25C-p in the binding of BI-2536 to PLK1, the interactions of the rest of the kinase inhibitors (Volasertib and Ro-3280) with the protein were investigated in presence of the phosphopeptide. For comparative purposes, the interaction between PLK1 and its substate, ATP, was also studied in the same

experimental conditions. As shown in Fig. 4 and S2, the titration of PLK1 with the kinase inhibitors and ATP quenches the fluorescence emission of the protein. As in the case of BI-2536, a weak emission with an isosbestic point at ~360 nm emerges upon Volasertib and Ro-3280 titration. Negative deviations in the Stern-Volmer plots were observed for both the inhibitors and the protein substrate, indicating the presence of inaccessible tyrosine residues in PLK1. The accessibility factors obtained according to equation 3 (f = 0.3) are comparable to the value previously determined for BI-2536 (see Table 1). The value of n calculated by using the equation 7 was within the range 0.65 - 0.80 according the single binding site reported for the substrate and the studied inhibitors [6,17,90]. Remarkably, the three kinase inhibitors showed higher affinity to PLK1 than the protein substrate. The binding constant determined for Ro-3280 is twofold higher than ATP and the constants found for BI-2536 and Volasertib are even larger. Besides, these results are also in agreement with the reported enzymatic IC_{50} values of the studied inhibitors. Thus, the binding constants determined for BI-2536 and Volasertib are comparable and in agreement with their IC_{50} values (0.83 and 0.87 nM, respectively) [17,32]. This finding is reasonable considering the high structural similarity of both compounds, particularly in the moiety that enters in the ATP pocket (*vide infra*); while the lowest binding constant was determined for Ro-3280 in consonance with its higher IC_{50} value (3 nm) [54,55]. Therefore, the studied compounds inhibit the enzymatic activity of PLK1 by binding to the active center with higher affinity than its native substrate. MD calculations allowed us to deepen into the intramolecular interactions involved in the binding of BI-2536 and Volasertib to PLK1. These results are compared to those obtained for the binding of ATP to the protein in the next section.

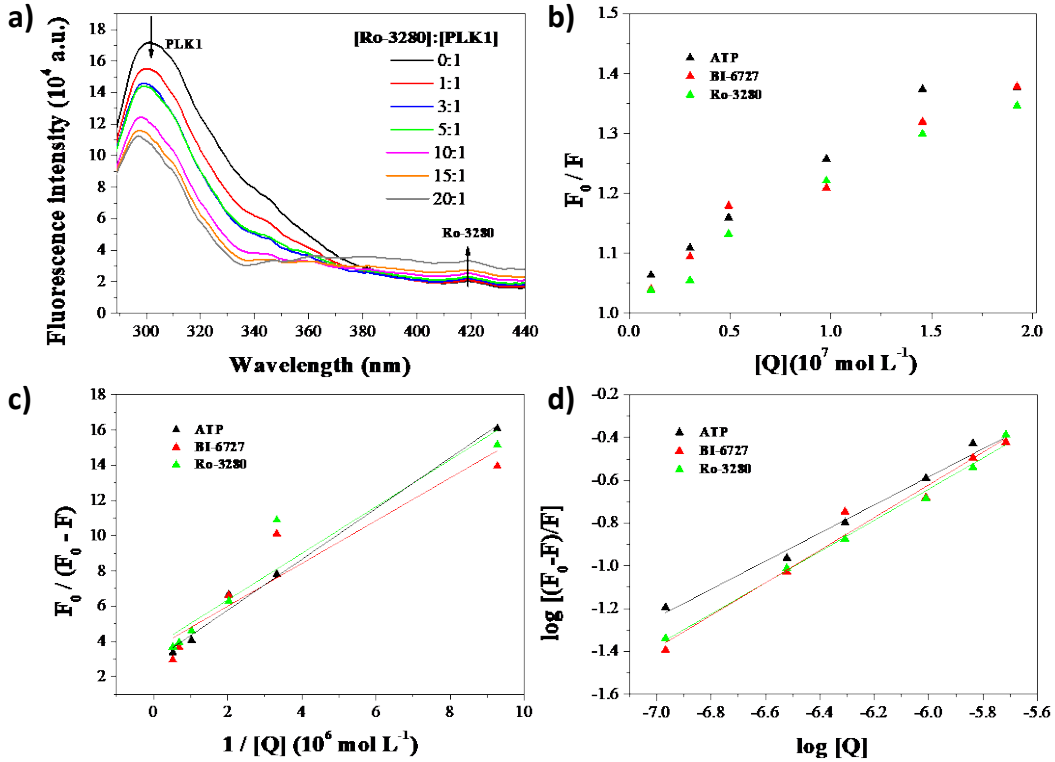

Fig. 4. a) Effect of Ro-3280 on the fluorescence emission spectrum of PLK1, along with Cdc25C-p in 1:1 stoichiometric proportion (T = 310 K, λ_{ex} = 275 nm). [PLK1] = [Cdc25C-p] = 0.1 μM; [Ro-3280] = 0.1–2.0 μM. b) Stern-Volmer plots obtained for Volasertib, Ro-3280 and ATP. c) Modified Stern-Volmer plots according equation 5 obtained for Volasertib, Ro-3280 and ATP. d) Plot of log [(F_0 − F) / F] *vs.* log [Q] at according equation 7 obtained for Volasertib, Ro-3280 and ATP.

3.3. MD analysis on the binding of PLK1 to the kinase inhibitors and its substrate

The MD trajectories have been used both to analyze the stability of the interactions established between each of the ligands and PLK1, and to obtain information using QM-MMGBSA [66] and K_{DEEP} [67] calculations on their relative binding free energies ($\Delta\Delta G_{bind}$). It is widely accepted that binding energies calculated by MMGB(PB)SA are not always in agreement with the values obtained experimentally, although its ability to rank the ligands on the basis of $\Delta\Delta G_{bind}$ is often quite good [91,92]. On the other hand, K_{DEEP}, has been designed to predict absolute binding free energies (ΔG_{bind}), although it only uses one structure and therefore does not take into account protein and ligand flexibility. Thus, clustering the trajectories in order to obtain representatives to be used as input for K_{DEEP} is expected to, at least in part, take also into account flexibility.

Table 3 shows the QM-MMGBSA calculated ΔG_{bind} values, which reproduce the experimental trend, i.e. the binding of BI-2536 to PLK1 is slightly more favored than the binding of Volasertib and significantly more favored than that of the native substrate. This result supports the values of the energy components shown in Table 4 that are summed to obtain each calculated ΔG_{bind}. The sum of the values obtained for the polar solvation term (ΔE_{GB}) and the PM6 term (ΔE_{SCF}) is positive in all cases, being the lowest value that computed for ATP. This is a reasonable result, considering the charge of the protein and the ligands (+12 for the protein; +1, +2 and -4 for BI-2536, Volasertib and ATP, respectively), and allows us to conclude that the lower binding affinity of ATP can be mainly explained through its worse van der Waals interactions as compared to those of BI-2536 and Volasertib. In addition, the van der Waals interactions are slightly better predicted for BI-2536, with respect to Volasertib, as a consequence of the change of a cyclopentyl ring with an isopropyl moiety, whose lower volume is directly related to lower hydrophobic interactions.

Table 3
QM-MMGBSA predicted binding free energies (ΔG_{bind}), in kcal mol^{-1}, for each of the MD runs obtained for the ligands studied. The average energy and its standard deviation are included.

Ligand	Run 1	Run 2	Run 3	Run 4	Run 5	Average	±2σ
BI-2536	-45.67	-45.61	-45.50	-43.10	-42.03	-44.38	0.67
Volasertib	-35.41	-34.76	-35.36	-35.37	-34.22	-35.02	0.37
ATP	-11.08	-12.35	-13.96	-10.45	-8.14	-11.20	0.76

Table 4
Energy components of ΔG_{bind} (see eq. 3), in kcal mol^{-1}, averaged over five independent MD runs (standard deviation is included).

	BI-2536		Volasertib		ATP	
	Average	±2σ	Average	±2σ	Average	±2σ
ΔE_{vdW}	-58.70	0.56	-57.58	0.29	-18.16	0.68
ΔE_{EEL}	0.00	0.00	0.00	0.00	0.00	0.00
ΔE_{GB}	-190.39	0.96	-457.88	1.14	913.49	2.02
ΔE_{SURF}	-6.57	0.18	-6.70	0.05	-6.21	0.20
ΔE_{SCF}	211.27	0.93	487.13	1.08	-900.31	2.07

The observed experimental trend can also be reproduced, with much less computational demand, using K_{DEEP} calculations, as shown in Table 5. It is worth emphasizing that the number of clusters found, even using two different approaches, is quite low, which correlates with the low RMSd obtained for the different trajectories (see Fig. S3). As will be described below, the ATP moiety moves inside the binding pocket establishing interactions which are somehow different from those previously described for BI-2536 [37], Volasertib [38] or ADP [69]. However, as can be seen when comparing the binding energies calculated for the experimental zebrafish PLK1/ADP system and for the modeled human PLK1/ATP system (in which ATP is located in the same place as ADP), the binding free energies are very similar. This result allows to hypothesize that the lower binding affinity of ATP, with respect to the kinase inhibitors, is mainly due to its weaker van der Waals interactions, which are not capable of compensating the electrostatic (hydrogen bond, charge) effects (ΔE_{SCF}). Actually, a π-π interaction, already described as important for binding and selectivity [37], established between Phe183 and the dihydropteridinone moiety of BI-2536 and Volasertib, does not have an equivalent in the experimental zebrafish PLK1/ADP nor modeled human PLK1/ATP. These kinds of interactions, whose contributions are proposed to be implicitly included in the van der Waals parameters of the Amber force field (among others) [93], exhibit an average ring

to ring distance of 3.7 Å / 4.4 Å during the MD trajectory for BI-2536 / Volasertib (3.9 Å for the experimental structures). The different structures obtained with the two essayed clustering options are shown in Fig. 5 and S4, while the hydrogen bond occupancy analysis is presented in Table S1.

Table 5
Binding free energies (ΔG_{bind}), in kcal mol^{-1}, as determined with K_{DEEP} for each cluster found. The binding free energies determined for the initial modeled ATP structure and the experimental zebrafish PLK1/ADP systems is also shown for comparison purposes.

		Members[c]	ΔG_{bind}
	Clustering 1[a]		
BI-2536	Cluster 1	12642	-10.45
Volasertib	Cluster 1	3154	-9.50
	Cluster 2	886	-8.35
	Cluster 3	762	-8.33
	Cluster 4	690	-8.33
	Cluster 5	638	-8.74
ATP	Cluster 1	11068	-6.36
	Initial modeled structure		-6.46
	Experimental ADP structure		-6.57
	Clustering 2[b]		
BI-2536	Cluster 1	3388	-11.43
Volasertib	Cluster 1	24400	-8.26
ATP	Cluster 1	5119	-7.53
	Cluster 2	1507	-6.90

[a] Clustering using all protein C_α atoms
[b] Clustering using all atoms within the binding pocket
[c] Number of snapshots composing each cluster

Thus, although with a low occupancy during the MD run, the canonical hydrogen bonds already described for BI-2536 between Cys133 and the $=N_\beta-$ group of the ligand and between Leu59 and the secondary amide group of the ligand, are found both with cpptraj and UCSF Chimera (see Fig. 5 and Table S1). The low occupancy for the Cys133/N_β H-bond is associated with small displacements of the ligand within the binding pocket, while for the Lue59/NH H-bond with the high rotational flexibility of that part of the molecule, which is mainly exposed to the solvent (see Fig. 5). As explained

above, the displacement followed by the ATP ligand within the binding pocket causes the equivalent Cys133 H-bond to break, while two strong H-bonds, with occupancies of 72.3% and 71.6% are predicted with Glu140 and Gly63, respectively. Another two newly H-bonds with lower occupancy are found with Arg136 (30.8%) and Lys178 (19.6%).

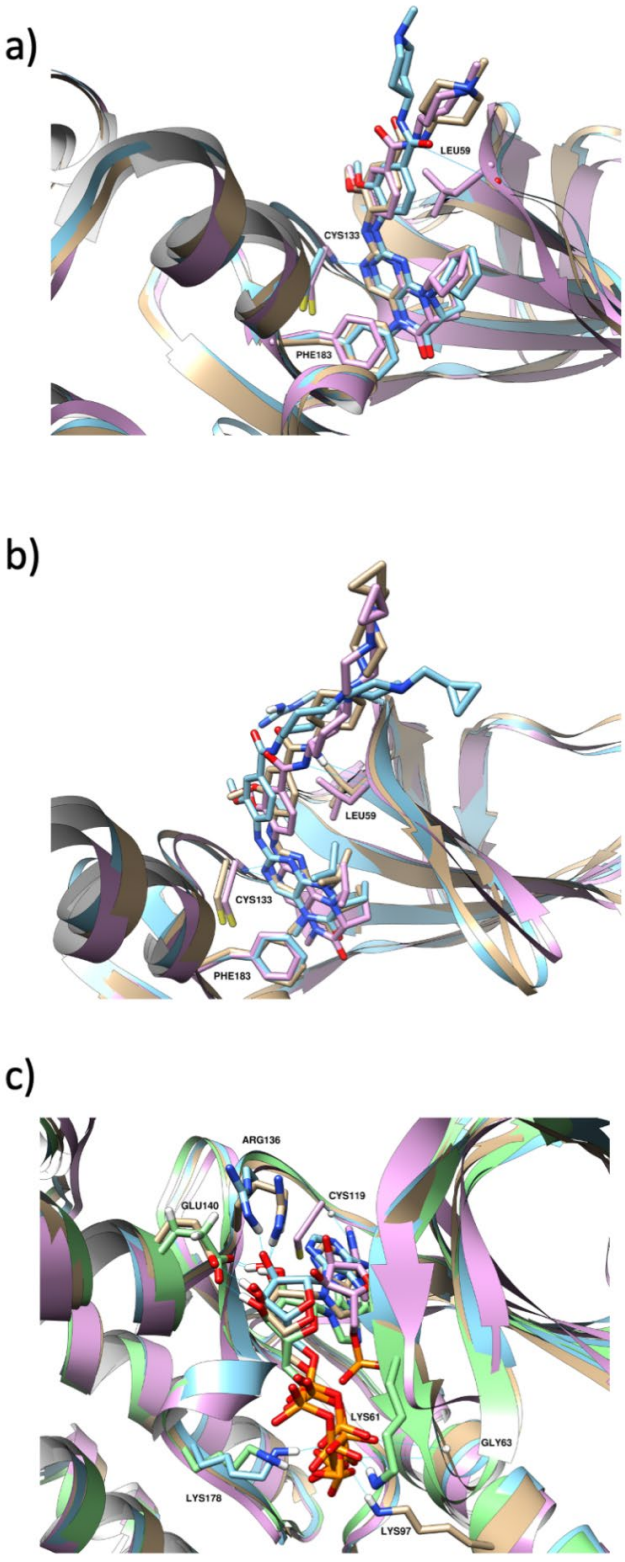

Fig. 5. Structures of the representatives of each cluster found showing the H-bonds and π-π interactions. Hydrogens apart from those implied in an H-bond are omitted for clarity. a) BI-2536, pink experimental structure, blue first cluster of clustering 1, brown first cluster of clustering 2. b) Volasertib, pink experimental structure, blue first cluster of clustering 1, brown first cluster of clustering 2. The remaining structures are shown in Fig. S4. c) ATP, pink experimental structure, green first cluster of clustering 1, brown first cluster of clustering 2, and blue second cluster of clustering 2.

Conclusions

The interactions of three kinase inhibitors (BI-2536, Volasertib and Ro-3280) with their pharmacological target PLK1 were studied by means of fluorescence spectroscopy and MD calculations. Results show kinase inhibitors form stable complexes with PLK1, and the presence of the phosphopeptide Cdc25C-p markedly increases their affinity by the protein. A single binding site was revealed and all the binding constants determined for the inhibitors are higher than those obtained for the protein substrate. The highest binding constants were found for BI-2536 and Volasertib in agreement with the reported enzymatic IC_{50} values. In addition, PLK1 exhibits a higher affinity for BI-2536 and Volasertib than for ATP based on the relative binding free energies calculated with both QM-MMGBSA and K_{DEEP}. Although ATP establishes more hydrogen bonds, the ΔG_{bind} values calculated for the substrate are smaller than for the studied inhibitors due to the weaker van der Waals interactions established with the protein. The discovery of new kinase inhibitor drugs with greater activity and specificity presents challenges associated with the development of new strategies and technologies that allow the efficient generation of highly optimized kinase inhibitors. This requires an understanding of the biology of kinases, the structural basis of kinase inhibitor selectivity, the direct relationship between the structure of the drug and the affinity for the active site and its consequent pharmacological activity. In this sense, we believe that results presented herein may be crucial to the ultimate goal of developing selective kinase inhibitors.

Acknowledgment

The authors would like to thank the “Universidad de Castilla-La Mancha” (2020-GRIN-29016), the Consejería de Economía y Conocimiento (Junta de Andalucía) (FQM-337), and the “Universidad de Jaén” (Acción 1) for financially supporting the research described in this article. Likewise, authors are grateful for the project DIPUAB-16-GARZONRUIZ financed jointly by the “Diputación de Albacete” and the “Universidad de Castilla-La Mancha”. P.J.P.-L. thanks the “Junta de Comunidades de Castilla-La Mancha” for his postdoctoral fellowship [2018/15132].

Conflict of interest

Authors deny any actual or potential conflict of interest.

Appendix A. Supplementary Data

Supplementary material: additional fluorescence spectra of PLK in absence and presence of drugs; additional information from molecular dynamic calculations.

References

[1] C.E. Sunkel, D.M. Glover, polo, a mitotic mutant of Drosophila displaying abnormal spindle poles., J. Cell Sci. 89 (Pt 1) (1988) 25–38.

[2] S. Llamazares, A. Moreira, A. Tavares, C. Girdham, B.A. Spruce, C. Gonzalez, R.E. Karess, D.M. Glover, C.E. Sunkel, polo encodes a protein kinase homolog required for mitosis in Drosophila., Genes Dev. 5 (1991) 2153–2165. https://doi.org/10.1101/gad.5.12a.2153.

[3] L.D. Berry, R.M. Golsteyn, H.A. Lane, K.E. Mundt, L. Arnaud, E.A. Nigg, The family of polo-like kinases, in: Prog. Cell Cycle Res., Springer US, Boston, MA, 1996: pp. 107–114. https://doi.org/10.1007/978-1-4615-5873-6_11.

[4] J. Xu, C. Shen, T. Wang, J. Quan, Structural basis for the inhibition of Polo-like kinase 1, Nat. Struct. Mol. Biol. 20 (2013) 1047–1053. https://doi.org/10.1038/nsmb.2623.

[5] S.M.A. Lens, E.E. Voest, R.H. Medema, Shared and separate functions of polo-like kinases and aurora kinases in cancer, Nat. Rev. Cancer. 10 (2010) 825–841. https://doi.org/10.1038/nrc2964.

[6] Z. Liu, Q. Sun, X. Wang, PLK1, A potential target for cancer therapy, Transl. Oncol. 10 (2017) 22–32. https://doi.org/10.1016/j.tranon.2016.10.003.

[7] B.C.M. van de Weerdt, R.H. Medema, Polo-Like Kinases: A Team in Control of the Division, Cell Cycle. 5 (2006) 853–864. https://doi.org/10.4161/cc.5.8.2692.

[8] M. Petronczki, M. Glotzer, N. Kraut, J.M. Peters, Polo-like Kinase 1 Triggers the Initiation of Cytokinesis in Human Cells by Promoting Recruitment of the RhoGEF Ect2 to the Central Spindle, Dev. Cell. 12 (2007) 713–725. https://doi.org/10.1016/j.devcel.2007.03.013.

[9] M. Petronczki, P. Lénárt, J.-M. Peters, Polo on the rise from mitotic entry to cytokinesis with Plk1., Dev. Cell. 14 (2008) 646–59. https://doi.org/10.1016/j.devcel.2008.04.014.

[10] V. Archambault, D.M. Glover, Polo-like kinases: conservation and divergence in their functions and regulation, Nat. Rev. Mol. Cell Biol. 10 (2009) 265–275. https://doi.org/10.1038/nrm2653.

[11] K.E. Mundt, R.M. Golsteyn, H.A. Lane, E.A. Nigg, On the Regulation and Function of Human Polo-like Kinase 1 (PLK1): Effects of Overexpression on Cell Cycle Progression, Biochem. Biophys. Res. Commun. 239 (1997) 377–385. https://doi.org/10.1006/bbrc.1997.7378.

[12] F. Eckerdt, J. Yuan, K. Strebhardt, Polo-like kinases and oncogenesis, Oncogene.

24 (2005) 267–276. https://doi.org/10.1038/sj.onc.1208273.

[13] P. Ramani, R. Nash, E. Sowa-Avugrah, C. Rogers, High levels of polo-like kinase 1 and phosphorylated translationally controlled tumor protein indicate poor prognosis in neuroblastomas, J. Neurooncol. 125 (2015) 103–111. https://doi.org/10.1007/s11060-015-1900-4.

[14] T.G. Tut, S.H.S. Lim, I.U. Dissanayake, J. Descallar, W. Chua, W. Ng, P. de Souza, J.-S. Shin, C.S. Lee, Upregulated Polo-Like Kinase 1 Expression Correlates with Inferior Survival Outcomes in Rectal Cancer, PLoS One. 10 (2015) e0129313. https://doi.org/10.1371/journal.pone.0129313.

[15] R. Zhang, H. Shi, F. Ren, H. Liu, M. Zhang, Y. Deng, X. Li, Misregulation of polo-like protein kinase 1, P53 and P21WAF1 in epithelial ovarian cancer suggests poor prognosis, Oncol. Rep. 33 (2015) 1235–1242. https://doi.org/10.3892/or.2015.3723.

[16] K. Strebhardt, A. Ullrich, Targeting polo-like kinase 1 for cancer therapy, Nat. Rev. Cancer. 6 (2006) 321–330. https://doi.org/10.1038/nrc1841.

[17] P. Schöffski, Polo-Like Kinase (PLK) Inhibitors in Preclinical and Early Clinical Development in Oncology, Oncologist. 14 (2009) 559–570. https://doi.org/10.1634/theoncologist.2009-0010.

[18] K. Strebhardt, Multifaceted polo-like kinases: Drug targets and antitargets for cancer therapy, Nat. Rev. Drug Discov. 9 (2010) 643–660. https://doi.org/10.1038/nrd3184.

[19] K.-Y. Cheng, The crystal structure of the human polo-like kinase-1 polo box domain and its phospho-peptide complex, EMBO J. 22 (2003) 5757–5768. https://doi.org/10.1093/emboj/cdg558.

[20] K.S. Lee, R.L. Erikson, Plk is a functional homolog of Saccharomyces cerevisiae

Cdc5, and elevated Plk activity induces multiple septation structures., Mol. Cell. Biol. 17 (1997) 3408–3417. https://doi.org/10.1128/MCB.17.6.3408.

[21] Y.-W. Qian, E. Erikson, J.L. Maller, Mitotic Effects of a Constitutively Active Mutant of the Xenopus Polo-Like Kinase Plx1, Mol. Cell. Biol. 19 (1999) 8625–8632. https://doi.org/10.1128/MCB.19.12.8625.

[22] O. Kelm, M. Wind, W.D. Lehmann, E.A. Nigg, Cell Cycle-regulated Phosphorylation of the XenopusPolo-like Kinase Plx1, J. Biol. Chem. 277 (2002) 25247–25256. https://doi.org/10.1074/jbc.M202855200.

[23] Y.-J. Jang, S. Ma, Y. Terada, R.L. Erikson, Phosphorylation of Threonine 210 and the Role of Serine 137 in the Regulation of Mammalian Polo-like Kinase, J. Biol. Chem. 277 (2002) 44115–44120. https://doi.org/10.1074/jbc.M202172200.

[24] B.C.M. van de Weerdt, M.A.T.M. van Vugt, C. Lindon, J.J.W. Kauw, M.J. Rozendaal, R. Klompmaker, R.M.F. Wolthuis, R.H. Medema, Uncoupling Anaphase-Promoting Complex/Cyclosome Activity from Spindle Assembly Checkpoint Control by Deregulating Polo-Like Kinase 1, Mol. Cell. Biol. 25 (2005) 2031–2044. https://doi.org/10.1128/MCB.25.5.2031-2044.2005.

[25] T. Matsumoto, P. -y. Wang, W. Ma, H.J. Sung, S. Matoba, P.M. Hwang, Polo-like kinases mediate cell survival in mitochondrial dysfunction, Proc. Natl. Acad. Sci. 106 (2009) 14542–14546. https://doi.org/10.1073/pnas.0904229106.

[26] A.E.H. Elia, P. Rellos, L.F. Haire, J.W. Chao, F.J. Ivins, K. Hoepker, D. Mohammad, L.C. Cantley, S.J. Smerdon, M.B. Yaffe, The Molecular Basis for Phosphodependent Substrate Targeting and Regulation of Plks by the Polo-Box Domain, Cell. 115 (2003) 83–95. https://doi.org/10.1016/S0092-8674(03)00725-6.

[27] A. Seki, J.A. Coppinger, C.-Y. Jang, J.R. Yates, G. Fang, Bora and the Kinase

Aurora A Cooperatively Activate the Kinase Plk1 and Control Mitotic Entry, Science (80-.). 320 (2008) 1655–1658. https://doi.org/10.1126/science.1157425.

[28] T.M. Johnson, R. Antrobus, L.N. Johnson, Plk1 Activation by Ste20-like Kinase (Slk) Phosphorylation and Polo-Box Phosphopeptide Binding Assayed with the Substrate Translationally Controlled Tumor Protein (TCTP) †, Biochemistry. 47 (2008) 3688–3696. https://doi.org/10.1021/bi702134c.

[29] S.-M. Yun, T. Moulaei, D. Lim, J.K. Bang, J.-E. Park, S.R. Shenoy, F. Liu, Y.H. Kang, C. Liao, N.-K. Soung, S. Lee, D.-Y. Yoon, Y. Lim, D.-H. Lee, A. Otaka, E. Appella, J.B. McMahon, M.C. Nicklaus, T.R. Burke Jr, M.B. Yaffe, A. Wlodawer, K.S. Lee, Structural and functional analyses of minimal phosphopeptides targeting the polo-box domain of polo-like kinase 1, Nat. Struct. Mol. Biol. 16 (2009) 876–882. https://doi.org/10.1038/nsmb.1628.

[30] B. García-Álvarez, G. De Cárcer, S. Ibañez, E. Bragado-Nilsson, G. Montoya, Molecular and structural basis of polo-like kinase 1 substrate recognition: Implications in centrosomal localization, Proc. Natl. Acad. Sci. U. S. A. 104 (2007) 3107–3112. https://doi.org/10.1073/pnas.0609131104.

[31] B. García-Álvarez, S. Ibañez, G. Montoya, Crystallization and preliminary X-ray diffraction studies on the human Plk1 Polo-box domain in complex with an unphosphorylated and a phosphorylated target peptide from Cdc25C, Acta Crystallogr. Sect. F Struct. Biol. Cryst. Commun. 62 (2006) 372–375. https://doi.org/10.1107/S1744309106007494.

[32] R.N. Murugan, J.-E. Park, E.-H. Kim, S.Y. Shin, C. Cheong, K.S. Lee, J.K. Bang, Plk1-targeted small molecule inhibitors: molecular basis for their potency and specificity, Mol. Cells. 32 (2011) 209–220. https://doi.org/10.1007/s10059-011-0126-3.

[33] Z. Yin, Y. Song, P.H. Rehse, Thymoquinone Blocks pSer/pThr Recognition by Plk1 Polo-Box Domain As a Phosphate Mimic, ACS Chem. Biol. 8 (2013) 303–308. https://doi.org/10.1021/cb3004379.

[34] W. Reindl, J. Yuan, A. Krämer, K. Strebhardt, T. Berg, Inhibition of Polo-like Kinase 1 by Blocking Polo-Box Domain-Dependent Protein-Protein Interactions, Chem. Biol. 15 (2008) 459–466. https://doi.org/10.1016/j.chembiol.2008.03.013.

[35] W. Reindl, J. Yuan, A. Krämer, K. Strebhardt, T. Berg, A Pan-Specific Inhibitor of the Polo-Box Domains of Polo-like Kinases Arrests Cancer Cells in Mitosis, ChemBioChem. 10 (2009) 1145–1148. https://doi.org/10.1002/cbic.200900059.

[36] N. Watanabe, T. Sekine, M. Takagi, J. Iwasaki, N. Imamoto, H. Kawasaki, H. Osada, Deficiency in Chromosome Congression by the Inhibition of Plk1 Polo Box Domain-dependent Recognition, J. Biol. Chem. 284 (2009) 2344–2353. https://doi.org/10.1074/jbc.M805308200.

[37] M. Kothe, D. Kohls, S. Low, R. Coli, G.R. Rennie, F. Feru, C. Kuhn, Y.H. Ding, Selectivity-determining residues in Plk1, Chem. Biol. Drug Des. 70 (2007) 540–546. https://doi.org/10.1111/j.1747-0285.2007.00594.x.

[38] D. Rudolph, M. Steegmaier, M. Hoffmann, M. Grauert, A. Baum, J. Quant, C. Haslinger, P. Garin-Chesa, G.R. Adolf, BI 6727, a polo-like kinase inhibitor with improved pharmacokinetic profile and broad antitumor activity, Clin. Cancer Res. 15 (2009) 3094–3102. https://doi.org/10.1158/1078-0432.CCR-08-2445.

[39] P. Lénárt, M. Petronczki, M. Steegmaier, B. Di Fiore, J.J. Lipp, M. Hoffmann, W.J. Rettig, N. Kraut, J.-M. Peters, The Small-Molecule Inhibitor BI 2536 Reveals Novel Insights into Mitotic Roles of Polo-like Kinase 1, Curr. Biol. 17 (2007) 304–315. https://doi.org/10.1016/j.cub.2006.12.046.

[40] M. Steegmaier, M. Hoffmann, A. Baum, P. Lénárt, M. Petronczki, M. Krššák, U.

Gürtler, P. Garin-Chesa, S. Lieb, J. Quant, M. Grauert, G.R. Adolf, N. Kraut, J.-M. Peters, W.J. Rettig, BI 2536, a Potent and Selective Inhibitor of Polo-like Kinase 1, Inhibits Tumor Growth In Vivo, Curr. Biol. 17 (2007) 316–322. https://doi.org/10.1016/j.cub.2006.12.037.

[41] J. Von Pawel, M. Reck, W. Digel, C. Kortsik, M. Thomas, N. Frickhofen, M. Schuler, B. Gaschler-Markefski, G. Hanft, M. Sebastian, Randomized phase II trial of two dosing schedules of BI 2536, a novel Plk-1 inhibitor, in patients with relapsed advanced or metastatic non-small-cell lung cancer (NSCLC), J. Clin. Oncol. 26 (2008) 8030–8030. https://doi.org/10.1200/jco.2008.26.15_suppl.8030.

[42] H.S. Pandha, A. Protheroe, J. Wylie, C. Parker, J. Chambers, S. Bell, G. Munzert, An open label phase II trial of BI 2536, a novel Plk1 inhibitor, in patients with metastatic hormone refractory prostate cancer (HRPC), J. Clin. Oncol. 26 (2008) 14547–14547. https://doi.org/10.1200/jco.2008.26.15_suppl.14547.

[43] K. Mross, C. Dittrich, W.E. Aulitzky, D. Strumberg, J. Schutte, R.M. Schmid, S. Hollerbach, M. Merger, G. Munzert, F. Fleischer, M.E. Scheulen, A randomised phase II trial of the Polo-like kinase inhibitor BI 2536 in chemo-naïve patients with unresectable exocrine adenocarcinoma of the pancreas – a study within the Central European Society Anticancer Drug Research (CESAR) collaborative network, Br. J. Cancer. 107 (2012) 280–286. https://doi.org/10.1038/bjc.2012.257.

[44] J. Fernández-Sainz, P.J. Pacheco-Liñán, J.M. Granadino-Roldán, I. Bravo, A. Garzón, J. Rubio-Martínez, J. Albaladejo, Binding of the anticancer drug BI-2536 to human serum albumin. A spectroscopic and theoretical study, J. Photochem. Photobiol. B Biol. 172 (2017) 77–87. https://doi.org/10.1016/j.jphotobiol.2017.05.016.

[45] F. Kratz, Albumin as a drug carrier: Design of prodrugs, drug conjugates and nanoparticles, J. Control. Release. 132 (2008) 171–183. https://doi.org/10.1016/j.jconrel.2008.05.010.

[46] G. Lambrinidis, T. Vallianatou, A. Tsantili-Kakoulidou, In vitro, in silico and integrated strategies for the estimation of plasma protein binding. A review, Adv. Drug Deliv. Rev. 86 (2015) 27–45. https://doi.org/10.1016/j.addr.2015.03.011.

[47] A.M. Merlot, D.S. Kalinowski, D.R. Richardson, Unraveling the mysteries of serum Albumin-more than just a serum protein, Front. Physiol. 5 (2014) 1–8. https://doi.org/10.3389/fphys.2014.00299.

[48] D. Rudolph, M. Steegmaier, M. Hoffmann, M. Grauert, A. Baum, J. Quant, P. Garin-Chesa, G. Adolf, Characterization of BI 6727, a novel Polo-like kinase inhibitor with a distinct pharmacokinetic profile and efficacy in a model of taxane-resistant colon cancer, Eur. J. Cancer Suppl. 6 (2008) 135. https://doi.org/10.1016/S1359-6349(08)72364-4.

[49] ClinicalTrials.gov. National Library of Medicine (US). 2013 Jan 29, Identifier NCT01721876, Volasertib in Combination With Low-dose Cytarabine in Patients Aged 65 Years and Above With Previously Untreated Acute Myeloid Leukaemia, Who Are Ineligible for Intensive Remission Induction Therapy (POLO-AML-2), (n.d.). https://www.clinicaltrials.gov/ct2/show/study/NCT01721876.

[50] Z. Zhang, P. Ma, Y. Jing, Y. Yan, M.-C. Cai, M. Zhang, S. Zhang, H. Peng, Z.-L. Ji, W. Di, Z. Gu, W.-Q. Gao, G. Zhuang, BET Bromodomain Inhibition as a Therapeutic Strategy in Ovarian Cancer by Downregulating FoxM1, Theranostics. 6 (2016) 219–230. https://doi.org/10.7150/thno.13178.

[51] L. Chen, J.L. Yap, M. Yoshioka, M.E. Lanning, R.N. Fountain, M. Raje, J.A.

Scheenstra, J.W. Strovel, S. Fletcher, BRD4 Structure–Activity Relationships of Dual PLK1 Kinase/BRD4 Bromodomain Inhibitor BI-2536, ACS Med. Chem. Lett. 6 (2015) 764–769. https://doi.org/10.1021/acsmedchemlett.5b00084.

[52] T. Noguchi-Yachide, BET Bromodomain as a Target of Epigenetic Therapy, Chem. Pharm. Bull. (Tokyo). 64 (2016) 540–547. https://doi.org/10.1248/cpb.c16-00225.

[53] J. Gohda, K. Suzuki, K. Liu, X. Xie, H. Takeuchi, J.I. Inoue, Y. Kawaguchi, T. Ishida, BI-2536 and BI-6727, dual Polo-like kinase/bromodomain inhibitors, effectively reactivate latent HIV-1, Sci. Rep. 8 (2018) 1–13. https://doi.org/10.1038/s41598-018-21942-5.

[54] S. Chen, D. Bartkovitz, J. Cai, Y. Chen, Z. Chen, X.-J. Chu, K. Le, N.T. Le, K.-C. Luk, S. Mischke, G. Naderi-Oboodi, J.F. Boylan, T. Nevins, W. Qing, Y. Chen, P.M. Wovkulich, Identification of novel, potent and selective inhibitors of Polo-like kinase 1, Bioorg. Med. Chem. Lett. 22 (2012) 1247–1250. https://doi.org/10.1016/j.bmcl.2011.11.052.

[55] N.-N. Wang, Z.-H. Li, H. Zhao, Y.-F. Tao, L.-X. Xu, J. Lu, L. Cao, X.-J. Du, L.-C. Sun, W.-L. Zhao, P.-F. Xiao, F. Fang, G.-H. Su, Y.-H. Li, G. Li, Y.-P. Li, Y.-Y. Xu, H.-T. Zhou, Y. Wu, M.-F. Jin, L. Liu, J. Ni, J. Wang, S.-Y. Hu, X.-M. Zhu, X. Feng, J. Pan, Molecular Targeting of the Oncoprotein PLK1 in Pediatric Acute Myeloid Leukemia: RO3280, a Novel PLK1 Inhibitor, Induces Apoptosis in Leukemia Cells, Int. J. Mol. Sci. 16 (2015) 1266–1292. https://doi.org/10.3390/ijms16011266.

[56] J.R. Lakowicz, Principles of fluorescence spectroscopy, 3rd Editio, Springer, New York, 2006.

[57] A. Garzón, I. Bravo, M.R. Carrión-Jiménez, Á. Rubio-Moraga, J. Albaladejo,

Spectroscopic study on binding of gentisic acid to bovine serum albumin, Spectrochim. Acta Part A Mol. Biomol. Spectrosc. 150 (2015) 26–33. https://doi.org/10.1016/j.saa.2015.05.045.

[58] M. Liu, T. Liu, Y. Shi, Y. Zhao, H. Yan, B. Sun, Q. Wang, Z. Wang, J. Han, Comparative study on the interaction of oxyresveratrol and piceatannol with trypsin and lysozyme: binding ability, activity and stability, Food Funct. 10 (2019) 8182–8194. https://doi.org/10.1039/C9FO01888C.

[59] M. Makarska-Bialokoz, Analysis of the binding interaction in uric acid - Human hemoglobin system by spectroscopic techniques, Spectrochim. Acta Part A Mol. Biomol. Spectrosc. 178 (2017) 47–54. https://doi.org/10.1016/j.saa.2017.01.063.

[60] M. Akram, I.A. Bhat, S. Anwar, A. Ahmad, Kabir-ud-Din, Biophysical perspective of the binding of ester-functionalized gemini surfactants with catalase, Int. J. Biol. Macromol. 88 (2016) 614–623. https://doi.org/10.1016/j.ijbiomac.2016.04.011.

[61] P. Qin, X. Pan, R. Liu, J. Qiu, X. Fang, Experimental and computational characterization on the binding of two fluoroquinolones to bovine hemoglobin, J. Mol. Recognit. 30 (2017) e2647. https://doi.org/10.1002/jmr.2647.

[62] L. Momeni, B. Shareghi, A.A. Saboury, S. Farhadian, F. Reisi, A spectroscopic and thermal stability study on the interaction between putrescine and bovine trypsin, Int. J. Biol. Macromol. 94 (2017) 145–153. https://doi.org/10.1016/j.ijbiomac.2016.10.009.

[63] M. Kothe, D. Kohls, S. Low, R. Coli, A.C. Cheng, S.L. Jacques, T.L. Johnson, C. Lewis, C. Loh, J. Nonomiya, A.L. Sheils, K.A. Verdries, T.A. Wynn, C. Kuhn, Y.H. Ding, Structure of the catalytic domain of human polo-like kinase 1, Biochemistry. 46 (2007) 5960–5971. https://doi.org/10.1021/bi602474j.

[64] D.A. Case Ross C Walker, T.E. Darden Junmei Wang Robert Duke, Amber 2018 , n.d. http://ambermd.org/contributors.html (accessed February 2, 2021).

[65] J.A. Maier, C. Martinez, K. Kasavajhala, L. Wickstrom, K.E. Hauser, C. Simmerling, ff14SB: Improving the Accuracy of Protein Side Chain and Backbone Parameters from ff99SB, J. Chem. Theory Comput. 11 (2015) 3696–3713. https://doi.org/10.1021/acs.jctc.5b00255.

[66] B.R. Miller, T.D. McGee, J.M. Swails, N. Homeyer, H. Gohlke, A.E. Roitberg, MMPBSA.py : An Efficient Program for End-State Free Energy Calculations, J. Chem. Theory Comput. 8 (2012) 3314–3321. https://doi.org/10.1021/ct300418h.

[67] J. Jiménez, M. Škalič, G. Martínez-Rosell, G. De Fabritiis, KDEEP: Protein-Ligand Absolute Binding Affinity Prediction via 3D-Convolutional Neural Networks, J. Chem. Inf. Model. 58 (2018) 287–296. https://doi.org/10.1021/acs.jcim.7b00650.

[68] E.F. Pettersen, T.D. Goddard, C.C. Huang, G.S. Couch, D.M. Greenblatt, E.C. Meng, T.E. Ferrin, UCSF Chimera - A visualization system for exploratory research and analysis, J. Comput. Chem. 25 (2004) 1605–1612. https://doi.org/10.1002/jcc.20084.

[69] R.A. Elling, R. V. Fucini, M.J. Romanowski, Structures of the wild-type and activated catalytic domains of Brachydanio rerio Polo-like kinase 1 (Plk1): Changes in the active-site conformation and interactions with ligands, Acta Crystallogr. Sect. D Biol. Crystallogr. 64 (2008) 909–918. https://doi.org/10.1107/S0907444908019513.

[70] G. Martínez-Rosell, T. Giorgino, G. De Fabritiis, PlayMolecule ProteinPrepare: A Web Application for Protein Preparation for Molecular Dynamics Simulations, J. Chem. Inf. Model. 57 (2017) 1511–1516.

https://doi.org/10.1021/acs.jcim.7b00190.

[71] J. Wang, R.M. Wolf, J.W. Caldwell, P.A. Kollman, D.A. Case, Development and testing of a general amber force field, J. Comput. Chem. 25 (2004) 1157–1174. https://doi.org/10.1002/jcc.20035.

[72] C.I. Bayly, P. Cieplak, W. Cornell, P.A. Kollman, A well-behaved electrostatic potential based method using charge restraints for deriving atomic charges: the RESP model, J. Phys. Chem. 97 (1993) 10269–10280. https://doi.org/10.1021/j100142a004.

[73] M. Janeček, M. Rossmann, P. Sharma, A. Emery, D.J. Huggins, S.R. Stockwell, J.E. Stokes, Y.S. Tan, E.G. Almeida, B. Hardwick, A.J. Narvaez, M. Hyvönen, D.R. Spring, G.J. McKenzie, A.R. Venkitaraman, Allosteric modulation of AURKA kinase activity by a small-molecule inhibitor of its protein-protein interaction with TPX2, Sci. Rep. 6 (2016) 28528. https://doi.org/10.1038/srep28528.

[74] W.L. Jorgensen, J. Chandrasekhar, J.D. Madura, R.W. Impey, M.L. Klein, Comparison of simple potential functions for simulating liquid water, J. Chem. Phys. 79 (1983) 926–935. https://doi.org/10.1063/1.445869.

[75] G. Vila-Julià, J.M. Granadino-Roldán, J.J. Perez, J. Rubio-Martinez, Molecular Determinants for the Activation/Inhibition of Bak Protein by BH3 Peptides, J. Chem. Inf. Model. 60 (2020) 1632–1643. https://doi.org/10.1021/acs.jcim.9b01047.

[76] J.J. Perez, M.S. Tomas, J. Rubio-Martinez, Assessment of the Sampling Performance of Multiple-Copy Dynamics versus a Unique Trajectory, J. Chem. Inf. Model. 56 (2016) 1950–1962. https://doi.org/10.1021/acs.jcim.6b00347.

[77] M. Ester, H.-P. Kriegel, J. Sander, X. Xu, A Density-Based Algorithm for

Discovering Clusters in Large Spatial Databases with Noise, in: Proc. 2nd Int. Conf. Knowl. Discov. Data Min., 1996: pp. 226–231. www.aaai.org (accessed February 2, 2021).

[78] V. Tsui, D.A. Case, Theory and applications of the generalized born solvation model in macromolecular simulations, Biopolymers. 56 (2000) 275–291. https://doi.org/10.1002/1097-0282(2000)56:4<275::AID-BIP10024>3.0.CO;2-E.

[79] G.D. Hawkins, C.J. Cramer, D.G. Truhlar, Parametrized models of aqueous free energies of solvation based on pairwise descreening of solute atomic charges from a dielectric medium, J. Phys. Chem. 100 (1996) 19824–19839. https://doi.org/10.1021/jp961710n.

[80] J. Weiser, P.S. Shenkin, W.C. Still, Approximate solvent-accessible surface areas from tetrahedrally directed neighbor densities, Biopolymers. 50 (1999) 373–380. https://doi.org/10.1002/(SICI)1097-0282(19991005)50:4<373::AID-BIP3>3.0.CO;2-U.

[81] H. Gohlke, D.A. Case, Converging free energy estimates: MM-PB(GB)SA studies on the protein-protein complex Ras-Raf, J. Comput. Chem. 25 (2004) 238–250. https://doi.org/10.1002/jcc.10379.

[82] J.J.P. Stewart, Optimization of parameters for semiempirical methods V: Modification of NDDO approximations and application to 70 elements, J. Mol. Model. 13 (2007) 1173–1213. https://doi.org/10.1007/s00894-007-0233-4.

[83] M.H. Gehlen, The centenary of the Stern-Volmer equation of fluorescence quenching: From the single line plot to the SV quenching map, J. Photochem. Photobiol. C Photochem. Rev. 42 (2020) 100338. https://doi.org/10.1016/j.jphotochemrev.2019.100338.

[84] M. Van De Weert, Fluorescence quenching to study protein-ligand binding:

Common errors, J. Fluoresc. 20 (2010) 625–629. https://doi.org/10.1007/s10895-009-0572-x.

[85] N.G. Zhdanova, E.A. Shirshin, E.G. Maksimov, I.M. Panchishin, A.M. Saletsky, V. V. Fadeev, Tyrosine fluorescence probing of the surfactant-induced conformational changes of albumin, Photochem. Photobiol. Sci. 14 (2015) 897–908. https://doi.org/10.1039/C4PP00432A.

[86] R. Starosta, F.C. Santos, R.F.M. de Almeida, Human and bovine serum albumin time-resolved fluorescence: Tryptophan and tyrosine contributions, effect of DMSO and rotational diffusion, J. Mol. Struct. 1221 (2020) 128805. https://doi.org/10.1016/j.molstruc.2020.128805.

[87] M. Jiang, M.X. Xie, D. Zheng, Y. Liu, X.Y. Li, X. Chen, Spectroscopic studies on the interaction of cinnamic acid and its hydroxyl derivatives with human serum albumin, J. Mol. Struct. 692 (2004) 71–80. https://doi.org/10.1016/j.molstruc.2004.01.003.

[88] M. Zhang, Q. Lv, N. Yue, H. Wang, Study of fluorescence quenching mechanism between quercetin and tyrosine-H2O2-enzyme catalyzed product, Spectrochim. Acta Part A Mol. Biomol. Spectrosc. 72 (2009) 572–576. https://doi.org/10.1016/j.saa.2008.10.045.

[89] X.Z. Feng, Z. Lin, L.J. Yang, C. Wang, C. li Bai, Investigation of the interaction between acridine orange and bovine serum albumin, Talanta. 47 (1998) 1223–1229. https://doi.org/10.1016/S0039-9140(98)00198-2.

[90] K.S. Lee, T.R. Burke, J.-E. Park, J.K. Bang, E. Lee, Recent Advances and New Strategies in Targeting Plk1 for Anticancer Therapy, Trends Pharmacol. Sci. 36 (2015) 858–877. https://doi.org/10.1016/j.tips.2015.08.013.

[91] J. Michel, J.W. Essex, Prediction of protein–ligand binding affinity by free

energy simulations: assumptions, pitfalls and expectations, J. Comput. Aided. Mol. Des. 24 (2010) 639–658. https://doi.org/10.1007/s10822-010-9363-3.

[92] S. Genheden, U. Ryde, The MM/PBSA and MM/GBSA methods to estimate ligand-binding affinities, Expert Opin. Drug Discov. 10 (2015) 449–461. https://doi.org/10.1517/17460441.2015.1032936.

[93] Z. Yang, Z. Wang, X. Tian, P. Xiu, R. Zhou, Amino acid analogues bind to carbon nanotube via π-π interactions: Comparison of molecular mechanical and quantum mechanical calculations, J. Chem. Phys. 136 (2012) 025103. https://doi.org/10.1063/1.3675486.